Supporting information to accompany the manuscript:

Multi-step microfluidic droplet processing: kinetic analysis of an in vitro translated enzyme

Linas Mazutis[a], Jean-Christophe Baret[a], Patrick Treacy[b], Yousr Skhiri[a], Ali Fallah Araghi[a] Michael Ryckelynck[a], Valérie Taly[a,b,*] and Andrew D. Griffiths[a,b,*]

[a] *Institut de Science et d'Ingénierie Supramoléculaire (ISIS), Université de Strasbourg, CNRS UMR 7006, 8 allée Gaspard Monge, 67083 Strasbourg Cedex, FR.*

[b] *Medical Research Council, Laboratory of Molecular Biology, Hills Road, Cambridge CB2 CQH, UK.*

Table of content of Supporting Information:

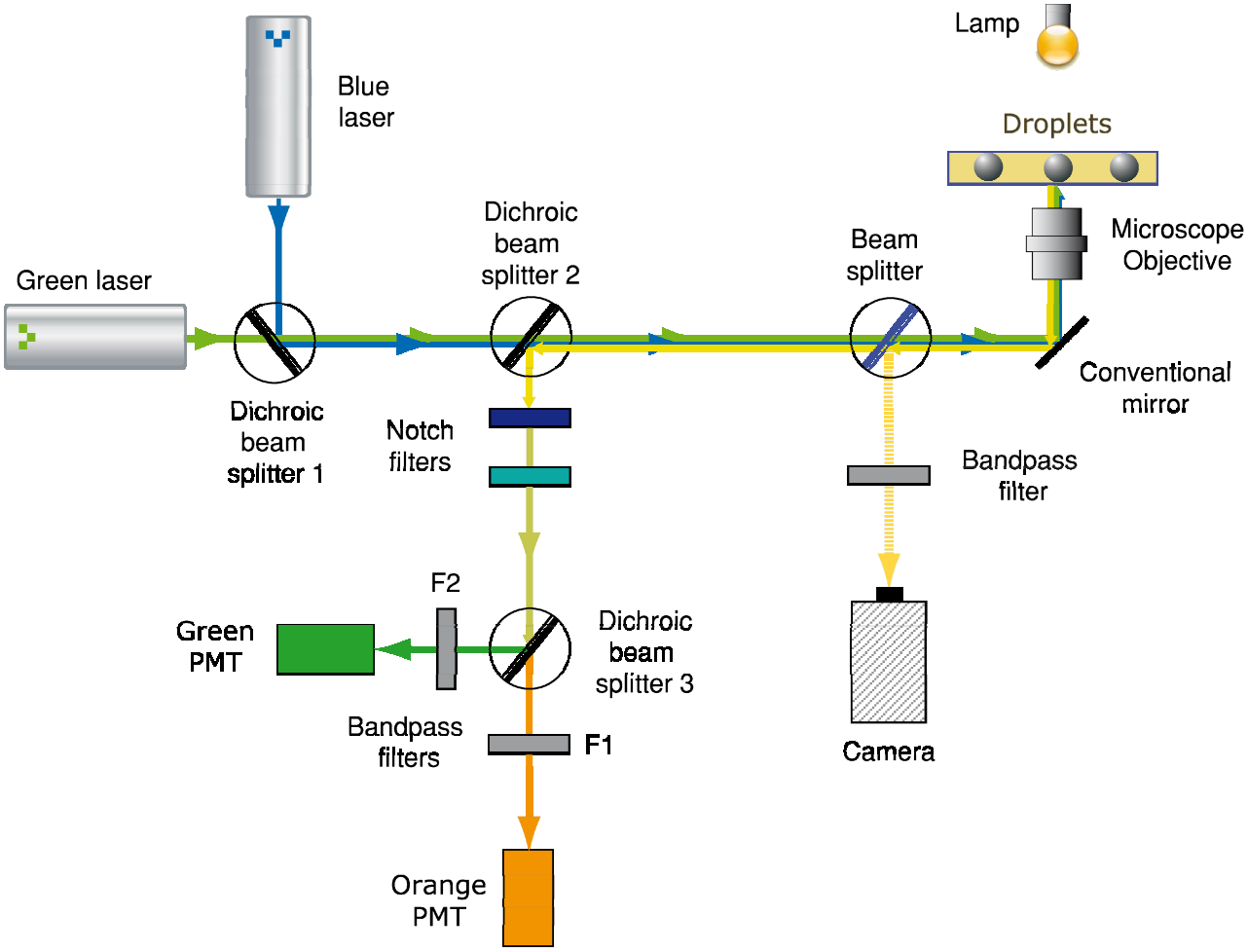

Figure S1. Schematic representation of the optical setup. The optical set-up comprised an Axiovert 200 inverted microscope (Carl Zeiss SAS) mounted on a vibration-dampening platform (Vibraplane, Kinetic Systems). Two solid-state lasers (25 mW) of 488 nm (Green) and 532 nm (Blue) wave-length (Newport-Spectraphysics) were fixed on the platform via heatsinks (Newport-Spectraphysics). The beams of the 488 and 532 nm lasers were shaped into the ~10 × ~150 µm wide line and a ~20 µm wide spot, respectively. The two laser beams were combined using a dichroic beam splitter 1 (LM01-503-25; Semrock Inc.) and guided to the side camera port of the microscope via a series of periscope assemblies (Thorlabs GmbH). The laser light was reflected up into an LD Plan Neofluar 40x/0.6 microscope objective (Carl Zeiss SAS) and focused in the microfluidic channel. A Phantom v4.2 high-speed digital camera (Vision Research) was mounted on the top camera port of the microscope to capture digital images during droplet production, fusion and re-injection. A 562/40 BrightLine® bandpass filter (Semrock Inc.) positioned in front of the camera protected the camera's sensor from reflected laser light. Light emitted from fluorescent droplets was captured by the objective and channeled back along the path of the laser into the system of periscope assemblies. The emitted light was separated from the laser beam by a 488/532/638 nm-wavelength transmitting dichroic beam splitter 2 (Di-T488/532/638-25x36x5.0; Semrock), filtered through the two notch filters (NF01-488-25 and NF01-532U-25; Semrock) and split between two photomultiplier tubes (PMTs) by a single-edge dichroic beam splitter 3 (FF562-Di02-25x36; Semrock). Transmitted light passed through a bandpass filter F1 (FF01-617/73-25; Semrock) to the Orange (Resorufin) PMT (H5784-20; Hamamatsu Photonics KK). Reflected light passed through another bandpass filter F2 (FF01-510/20-25; Semrock) to the Green (Fluorescein) PMT (H5784-20; Hamamatsu Photonics KK). The signal output from the PMT was analysed using a PCI-7831R Multifunction Intelligent DAQ card (National Instruments Corporation) executing a program written in LabView 8.2 (FPGA module, National Instruments Corporation), which allowed the identification of droplets by peaks in fluorescence, as well as the width of each droplet. The data acquisition rate for the system was 100 kHz. .

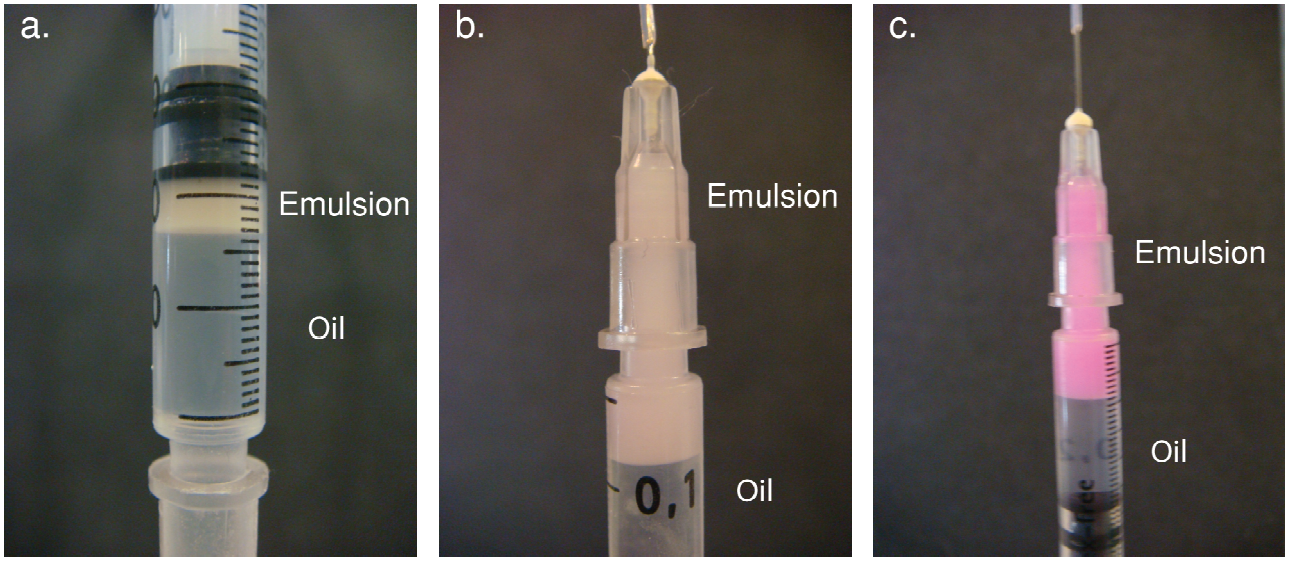

Figure S2. Emulsion storage off-chip. Digital photographs (Fujifilm, Finepix camera) of emulsions collected into latex-free 1 mL syringes. (a) IVT droplets after incubation at 30ºC for 6 hours; (b) IVT droplets fused with Assay droplets after collection at 4ºC and (c) IVT droplets fused with Assay droplets after incubation at 30ºC for 3 hours.

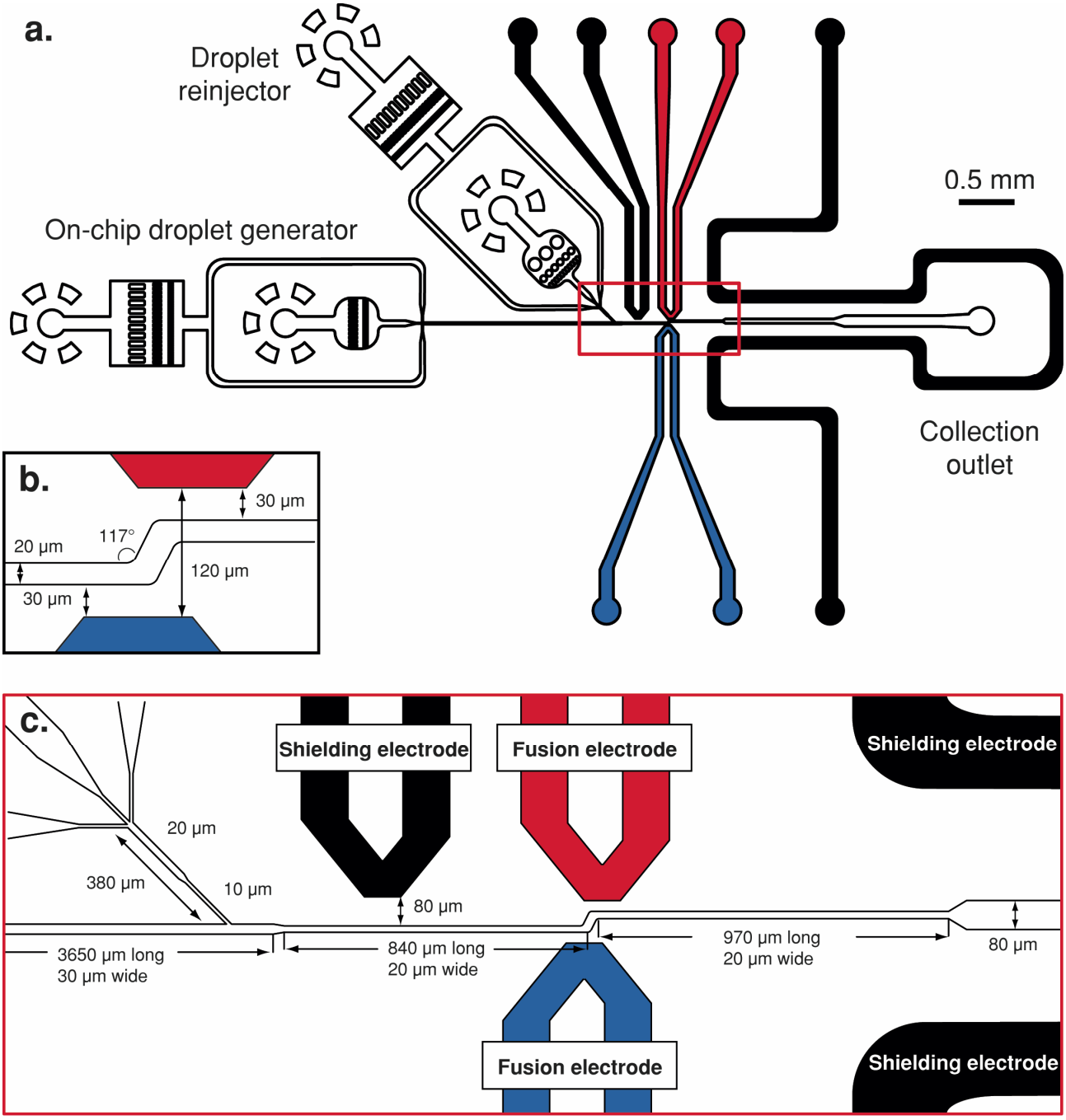

Figure S3. Design of the droplet electro-coalescence device. (**a**) Design of the complete droplet electro-coalescence device. (**b**) Magnified view of the electro-coalescence region. (**c**) Magnified view of the red box from panel **a**.

Design and optimization of the electro-coalescence device

The electro-coalescence device described in **Figure S3** was created after a series of optimizations. (**1**) We observed that droplet pairing was most efficient if the larger droplets produced on-chip were pinched in the pairing module, whereas the smaller re-injected droplets were unpinched. Therefore, we used a 30 x 20 μm^2 cross-section channel for on-chip droplet production, followed by a 20 x 20 μm^2 cross-section channel for pairing in which droplets larger than 8 pL (25 μm in spherical diameter) become pinched (**Figure S3**). (**2**) The length of the pairing channel was also important. We observed that in a pairing channel longer than 1.5 mm the spacing between individual droplet pairs (i.e. an 8 pL on-chip droplet paired with a 2 pL droplet) decreased leading to the formation of clusters containing multiple droplets and a higher number of undesirable fusion events. The optimal length of the pairing channel was 840 μm. (**3**) We observed that a Ψ-shaped reinjection module reduced the undesirable break-up of droplets during emulsion reinjection compared to a classical flow-focusing junction. In the Ψ-shaped reinjection module the two channels for the continuous phase are connected to the emulsion reinjection channel at an angle of 45º degrees, while in a classical flow-focusing junction they are connected at 90º. We believe that this decrease in the angle helps to reduce the shear force during the reinjection and spacing of individual droplets. (**4**) The shape of the fusion electrodes was not crucially important. However, the electrodes had to be placed in close proximity to the main channel so that the ac electrical field between them could effectively destabilize the interface between two droplets. We placed each electrode 30 μm away from the main channel. The optimal electrical field across the fusion electrodes, which were spaced apart by 120 μm, was generated at 400-800 V and 30 kHz. Below 300 V droplets did not coalesce and above 800 V droplets split producing smaller satellite droplets. The operating frequency of the electro-coalescence device was approximately 3000 fusion events per second. We have not observed malfunctioning of the system if droplets were fused at lower frequencies (<2 kHz). Operation of the microfluidic device above 4 kHz was not tested. (**5**) Since the distance between the positive electrode and the reinjection module and the collection module were relatively small (~1 mm) electrical fields could cause uncontrolled coalescence during emulsion reinjection and collection. To avoid undesirable coalescence it was necessary to incorporate two additional shielding electrodes: one for the protection of the IVT emulsion during reinjection and second for the protection of the fused droplets during collection off-chip. These shielding electrodes were grounded and therefore imposed a zero voltage boundary condition for the rest of the chip. Each shielding electrode was placed 80 μm away from the main channel as indicated in the **Figure S3**.

Supplementary movies:

Movie M1 shows 2 pL IVT droplet production. The device contains a Ψ-shaped connection, in which two aqueous streams are merged and emulsified using 10 μm wide flow focusing junction. The fluorinated HFE-7500 oil used to produce droplets contained 3% (w/w) EA-surfactant. The droplets were collected at the exhaust.

Movie M2 shows IVT emulsion re-injection after 6 hours of incubation off-chip. The re-injection rate was 20 μL/hr for the IVT emulsion and 180 μL/hr for the carrier oil used to space droplets. The carrier oil was FC40 with 3% (w/w) EA-surfactant.

Movie M3 shows droplet re-injection, pairing and electro-coalescence. 2 pL IVT droplets were re-injected at 20 μL/hr and spaced by carrier oil at 180 μL/hr. 10 pL Assay droplets were generated by the on-chip droplet generation module using 100 μL/hr for the aqueous phase and 200 μL/hr for the carrier oil. Carrier oil was FC40 with 3% (w/w) EA-surfactant. The fused droplets were collected at the exhaust.

Movie M4 shows the fusion module during electro-coalescence of 2 pL IVT droplets with 10 pL Assay droplets.

Movie M5 shows the fused droplets after electro-coalescence, collection off-chip and re-injection. Re-injection rate was 20 μL/hr for the emulsion and 120 μL/hr for the carrier oil used to space droplets.